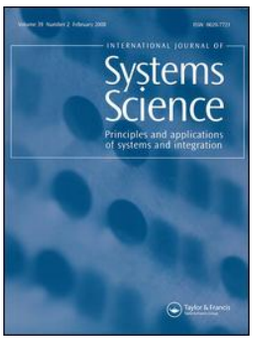

International Journal of Systems Science

ISSN: 0020-7721 (Print) 1464-5319 (Online) Journal homepage: http://www.tandfonline.com/loi/tsys20

Non-zero set-point affine feedback control of impulsive systems with application to biomedical processes

Pablo S. Rivadeneira & Alejandro H. González

To cite this article: Pablo S. Rivadeneira & Alejandro H. González (2018): Non-zero set-point affine feedback control of impulsive systems with application to biomedical processes, International Journal of Systems Science, DOI: 10.1080/00207721.2018.1533049

To link to this article: https://doi.org/10.1080/00207721.2018.1533049

Published online: 16 Oct 2018.

INTERNATIONAL JOURNAL OF SYSTEMS SCIENCE
https://doi.org/10.1080/00207721.2018.1533049

Non-zero set-point affine feedback control of impulsive systems with application to biomedical processes

Pablo S. Rivadeneira [a,b] and Alejandro H. González[b]

[a]Universidad Nacional de Colombia, Facultad de Minas, Grupo GITA, Medellín, Colombia; [b]Instituto de Desarrollo Tecnológico para la Industria Química INTEC - CONICET, Santa Fe, Argentina

ABSTRACT

Linear impulsive systems have been extensively studied in the last decades, mainly in the field of biomedical research. However, a proper characterisation of the equilibria of such a systems - when they are out of the origin - and its use by optimising control strategies is still a matter of discussion. In this work, a novel characterisation of the system equilibria and invariant regions - derived from the definition of two underlying discrete-time systems - is given, and based on this characterisation impulsive affine feedback control strategies for non-zero set-points are designed. The closed-loop performance and benefits of the strategies are assessed through two biomedical examples: the Lithium ions distribution in the human body and the HIV treatment.

ARTICLE HISTORY
Received 11 September 2017
Accepted 16 September 2018

KEYWORDS
Impulsive systems; non-zero regulation; feedback control; impulsive invariant sets; drug administration

1. Introduction

Impulsive control systems (ICS) - i.e. those which show first order discontinuities in the time evolution of the variables at certain times of a given sequence, and free responses between these times - have received great attention in the last decades. A typical application is in the field of biomedical research, where the drug intake is modelled as impulses in the treatment of several human diseases, as it was stated in the seminal work of Bellman (1971). Just to enumerate some remarkable examples, we mention the human immunodeficiency virus (HIV) (Chang, Astolfi, Moog, & Rivadeneira, 2014; Luo, Piovoso, Martinez-Picado, & Zurakowski, 2011; Rivadeneira & Moog, 2012), the malaria (Chang, Astolfi, & Shim, 2011), the influenza with co-infections (Boianelli, Sharma-Chawla, Bruder, & Hernandez-Vargas, 2016), the tumour-bearing (Chen, Kirkby, & Jena, 2012) and the type I diabetes (Huang, Li, Song, & Guo, 2012; Rivadeneira, Ferramosca, & Gonzalez, 2016).

However, in spite of its potential to describe such a significant dynamics, the regulation to non-zero set-points - which is usually the case - has received little attention in the literature, since the only one formal equilibrium of a typical impulsive system (particularly the linear ones) is the origin. For instance, in Chen and Tian (2013), the regulation problem is approached by using Lyapunov function methods and sufficient conditions are given for both, the solvability of the tracking problem and the output-tracking offset-free property. However, it is assumed that the output reference (an equilibrium) is at the origin; otherwise, the methodology does not work properly. In Fraga (2013), an impulsive feedback is studied and some invariance notions are introduced, but the regulation to the origin is still the control framework. In Wei, Zhang, and Chen (2013), an impulsive state feedback is designed and tested in the context of a cheese whey fermentation application. The work deals with non zero set-point regulation problems, but the results cannot be extended to general impulsive systems. Recently, in Tang and Xiao (2016), an interesting application of an impulsive feedback control is given. The idea is to combine surgery and immunotherapy in the cancer treatment context. This work illustrates the importance of this type of control.

In Sopasakis, Patrinos, Sarimveis, and Bemporad (2015) a version of model predictive control (MPC) for ICS has been developed, with an application to the dosing of intravenous bolus of Lithium ions upon oral intake (Ehrlich, Clausen, & Diamond, 1980; Pierce & Schumitzky, 1976). The strategy also covers the problem to steer a linear ICS (LICS) to a zone defined by a 'therapeutic window', which does not necessarily include the origin. The formulation is based on a polytopic invariant

CONTACT Pablo S. Rivadeneira psrivade@santafe-conicet.gov.ar Universidad Nacional de Colombia, Facultad de Minas, Grupo GITA, Carrera 80, #65-224 Medellín, Colombia; Instituto de Desarrollo Tecnológico para la Industria Química INTEC - CONICET, Güemes 3450, Santa Fe, Argentina

target set characterisation, which is difficult to compute and prevents its use in most application cases. An easier method to compute the target sets is provided in Rivadeneira, Ferramosca, and González (2015), also in the context of Impulsive MPC. These strategies were applied to the diabetes type 1 problem, in Rivadeneira et al. (2016)), and to the HIV treatment, in Rivadeneira, Caicedo, Ferramosca, and González. (2017), where preliminary concepts about non-zero set-point regulation are also established.

In this paper, the following contributions are presented. Firstly, a complete dynamic characterisation of linear ICS is developed and discussed. Non-zero equilibrium regions are characterised by means of two underlying linear discrete-time systems which naturally arise when the time instants before and after the impulsive time are considered. Secondly, the conditions to establish the impulsive stability of the new equilibria are described, where the free responses of the impulsive scheme are also taken into account. Finally, two efficient feedback controllers that take advantage of the latter impulsive characterisation are given, being the second one an optimisation-based strategy. The performance of the strategies is illustrated by means of two biomedical applications (lying in the central problem of scheduling of medicaments), as they are the Lithium ions distribution in the human body and the HIV treatment.

The paper is organised as follows. After the Introduction, some preliminaries are given in Section 2. Then, the novel theoretical characterisation of ICS is introduced in Section 3. Based on this latter study, two new control strategies for impulsive systems are developed in Section 4. The results of applying these strategies to two case-studies are shown in Section 5, while the last Section is devoted to present the conclusions and perspectives.

1.1. Notation

$\mathbb{N}$, $\mathbb{R}$, $\mathbb{R}^n$ and $\mathbb{R}^{n\times m}$ denote the sets of non-negative integers, reals, column vectors of length n and n by m matrices, respectively. $I_n \in \mathbb{R}^{n\times n}$ is the identity matrix. Given a matrix M,$\rho(M)$ denotes its spectral radius (see Ortega, 1987). Given a function $f : \mathbb{R} \to \mathbb{R}^n$, $f(a^+) \triangleq \lim_{t\to a^+} f(t)$, i.e. $f(a^+)$ is the limit of $f(t)$ when t approaches a from the right. $\|f\|$ represents any norm on functions (for instance, $\|f(t)\| \triangleq \sup_{t\in(0,T]} f(t)$). The convex hull of a collection of sets $\mathcal{V}_i$, $i = 1, 2, \ldots, k$ (i.e. the smallest convex set containing all the sets) is denoted as $\mathrm{ch}\{\mathcal{V}_1, \mathcal{V}_2, \ldots, \mathcal{V}_k\}$. Given a nonempty closed set $\mathcal{V}$, the distance from a point x to $\mathcal{V}$ is denoted by $dist_{\mathcal{V}}(x) \triangleq \min_{y\in\mathcal{V}} \|y - x\|$, where $\|\cdot\|$ is the Euclidean norm.

2. Preliminaries

The class of dynamic systems of interest in this paper consists of a set of linear impulsive first-order differential equations of the form

$$\begin{aligned} \dot{x}(t) &= A_c x(t), \quad x(0) = x_0, && t \neq \tau_k, \\ x(\tau_k^+) &= A_d x(\tau_k) + Bu(\tau_k), && k \in \mathbb{N}, \end{aligned} \tag{1}$$

where the independent variable $t \in \mathbb{R}$ denotes time, τ_k, $k \in \mathbb{N}$, denotes the impulse time instants, $x \in \mathcal{X} \subseteq \mathbb{R}^n$ denotes the state vector and $u \in \mathcal{U} \subseteq \mathbb{R}^m$ denotes the impulsive control inputs. It is assumed that the state trajectories are left continuous, i.e. $\lim_{t\to a^-} x(t) = x(a)$. Matrices $A_c \in \mathbb{R}^{n\times n}$ and $A_d \in \mathbb{R}^{n\times n}$ are the continuous and discrete transition matrices, while $B \in \mathbb{R}^{n\times m}$ is the impulsive input matrix. Notice that when $A_d = I_n$, the first order discontinuities of the solution are exclusively due to the controls $u(\tau_k)$. Furthermore, as part of the system description, a target state set $\mathcal{X}^{Tar} \subset \mathcal{X}$ is defined, which is the region where the system is desired to be driven to and kept.

Let $t_0 = 0$ be the initial time and $\mathcal{T} = \{0, \tau_1, \ldots, \tau_k, \ldots\}$ a set of time instants, with $T_i \triangleq \tau_{i+1} - \tau_i$. The state response of system (1) for $\tau_k < t \leq \tau_{k+1}$, with k impulses applied to the system, is described by:

$$x(t) = \Phi(t, 0)x_0 + \sum_{j=1}^{k} \Phi(t, \tau_j)Bu(\tau_j), \tag{2}$$

where the state transition matrix Φ is given by:

$$\Phi(t, \tau_j) = \mathrm{e}^{A_c(t-\tau_k)} \prod_{i=j+1}^{k} M_{k-i}, \tag{3}$$

and $M_i \triangleq A_d\, \mathrm{e}^{A_c T_i}$. The state transition matrix is invertible for all $t \in [0, \infty)$ if and only if the matrix A_d is invertible, and in this case, $\Phi(0, t) = \Phi^{-1}(t, 0)$. In this work, however, it will be assumed for simplicity that the time period is constant. This way, the impulse time instants τ_k are given by $\tau_k = kT$, $k \in \mathbb{N}$, being T the constant time period.

Let $\mathbf{u}$ be an input sequence of length N,

$$\mathbf{u} = \{u(\tau_1), u(\tau_2), \ldots, u(\tau_N)\}, \tag{4}$$

drawn from $\mathcal{U}$. And let $\varphi(t; x_0, \mathbf{u})$ be the solution to system (1), with $\varphi(0; x_0, \mathbf{u}) = x_0$. Let $t > 0$ and let τ_k be the largest impulse time such that $\tau_k \leq t$, with $k \leq N$. Then, for $\tau_k < t \leq \tau_{k+1}$ it is $\varphi(t; x_0, \mathbf{u}) = \mathrm{e}^{A_c(t-\tau_k)}\varphi(\tau_k^+; x_0, \mathbf{u})$,

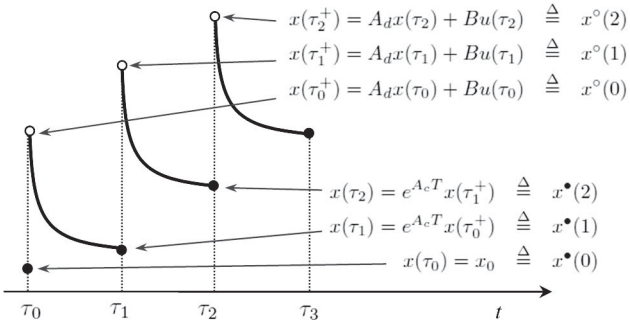

Figure 1. Typical state system evolution.

which can be expressed as

$$x(t) = \varphi(t; x_0, \mathbf{u}) \triangleq \mathrm{e}^{A_c(t-\tau_k)} \left(M^k x_0 + \sum_{j=1}^{k} M^{k-j} B u(\tau_j) \right) \tag{5}$$

where now $M = A_d\, \mathrm{e}^{A_c T}$. Notice that if $B \neq 0$ and $A_d = I$, the state response equation becomes

$$x(t) = \mathrm{e}^{A_c t} \left(x_0 + \sum_{j=1}^{k} \mathrm{e}^{-A_c \tau_j} B u(\tau_j) \right), \tag{6}$$

which agrees with the solution of the system presented in Yang (2001). A typical state evolution of an impulsive system is shown in Figure 1.

Let $\kappa(\cdot)$ be a control law, in such a way that $u(\tau_k) = \kappa(x(\tau_k))$, for $k \in \mathbb{N}$. Then, the closed-loop impulsive system is described by:

$$\dot{x}(t) = A_c x(t), \quad x(0) = x_0, \quad t \neq \tau_k, \tag{7a}$$

$$x(\tau_k^+) = A_d x(\tau_k) + B\kappa(x(\tau_k)), \quad k \in \mathbb{N}. \tag{7b}$$

This way, the closed-loop trajectory is denoted by $x(t) = \phi_{cl}(t; x_0, \kappa(\cdot))$, for $t \geq 0$, with $\phi_{cl}(0; x_0, \kappa(\cdot)) = x_0$, and clearly, the 'jump' depends now only on the state.

3. Dynamic characterisation

3.1. Underlying discrete-time systems

The impulsive control system given by Equation (1) is a hybrid system characterised by an autonomous and continuous part - modelled by differential equations - and by a discrete sequence where the state has discontinuities of the first kind. This discrete sequence is represented by the 'algebraic equation' in (1), and relates the state at time τ_k^+ with the state and the impulsive input at times τ_k. However, it is possible to expand this characterisation by defining two discrete-time systems, obtained by sampling the LICS at τ_k and τ_k^+, respectively, for $k \in \mathbb{N}$. This way, the so defined primary and secondary underlying discrete systems, UDS, are given by

$$x(\tau_{k+1}) = \mathrm{e}^{A_c T} \overbrace{[A_d x(\tau_k) + Bu(\tau_k)]}^{x(\tau_k^+)}, \tag{8}$$

$$x(\tau_k^+) = A_d \overbrace{\mathrm{e}^{A_c T} x(\tau_{k-1}^+)}^{x(\tau_k)} + Bu(\tau_k), \tag{9}$$

respectively, where $x(\tau_{-1}^+) \triangleq \mathrm{e}^{-A_c T} x(\tau_0)$, and the inputs $u(\tau_k)$ are assumed to be known at time instants τ_k^+.

If matrices $A^\circ \triangleq A_d\, \mathrm{e}^{A_c T}$, $A^\bullet \triangleq \mathrm{e}^{A_c T} A_d$, $B^\circ \triangleq B$ and $B^\bullet \triangleq \mathrm{e}^{A_c T} B$ are defined, and $u^\circ(j+1) = u^\bullet(j)$, for $j \geq 0$, the primary and secondary UDS can be written as:

$$x^\bullet(j+1) = A^\bullet x^\bullet(j) + B^\bullet u^\bullet(j), \quad x^\bullet(0) = x(\tau_0), \tag{10}$$

$$x^\circ(j+1) = A^\circ x^\circ(j) + B^\circ u^\circ(j), \quad x^\circ(0) = x(\tau_0^+), \tag{11}$$

respectively. The initial conditions of these two systems are related by $x^\circ(0) = x(\tau_0^+) = A_d x(\tau_0) + Bu(\tau_0) = A_d x^\bullet(0) + Bu(\tau_0)$, while the inputs fulfil $u^\circ(j+1) = u^\bullet(j)$, which means that the two discrete time systems share the same control input. These two systems describe the original system (1) at the impulsive times, τ_k, and an instant after this time, when the jump has already occurred (τ_k^+). That is why (11) and (10) are called the underlying discrete-time systems of the ICS (1).

Remark 3.1: The continuous time response of the ICS (1), for a period $(\tau_k, \tau_{k+1}]$, and a given state $x(\tau_k)$, can be described by

$$x(t) = A^\bullet(t) x(\tau_k) + B^\bullet(t) u(\tau_k), \quad \text{for } t \in (0, T] \tag{12}$$

where $A^\bullet(t) \triangleq \mathrm{e}^{A_c t} A_d$ and $B^\bullet(t) \triangleq \mathrm{e}^{A_c t} B$. This way, the continuous time response for each period is computed (characterised) by a linear map in which the matrices are time varying matrices.

3.2. Impulsive system equilibrium set characterisation

If matrices A_c and B are assumed to be full rank, the only formal equilibrium point of the ICS (1) is given by $(u_s, x_s) = (0, 0)$, which is the only pair verifying $\dot{x} = 0$ and $x(\tau_k^+) = x(\tau_k)$. However, by extending the concept of equilibrium to the one of invariance, it is possible to find some generalisation that accounts for equilibrium/invariant entities out of the origin (Sopasakis et al., 2015).

Definition 3.1 (Generalised control equilibrium set of ICS): Consider a ICS (1), a period T and a non-empty

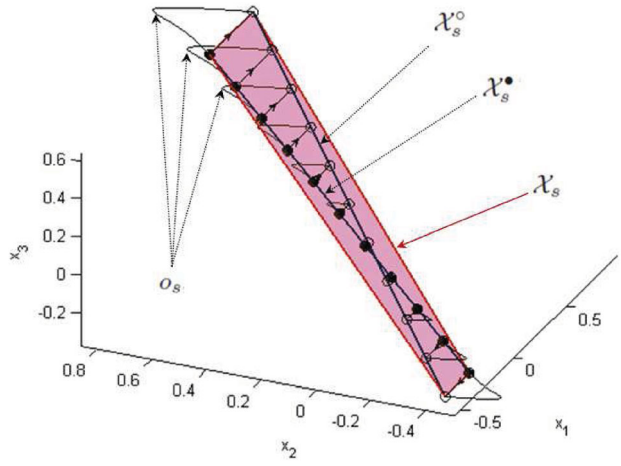

Figure 2. Set $\mathcal{X}_s$ into a subspace of dimension 2 in $\mathbb{R}^3$, sets $\mathcal{X}_s^\circ$ and $\mathcal{X}_s^\bullet$, and equilibrium orbitso_s of a simulated ICS.

convex set Ω. A set $\mathcal{X}_s \in \mathcal{X}$ is a generalised control equilibrium set with respect to Ω if for each $x_s \in \mathcal{X}_s$ there exists an input $u_s = u_s(x_s) \in \mathcal{U}$ such that

$$\phi(T; x_s, u_s(x_s)) \in \mathcal{X}_s, \tag{13}$$

$$o_s(x_s, u_s(x_s)) \subseteq \Omega, \tag{14}$$

where $o_s(x_s, u_s) \triangleq \{\phi(t; x_s, u_s),\ t \in (0, T]\}$. The set $\{u_s(x_s) \in \mathcal{U} : x_s \in \mathcal{X}_s\}$ is denoted as $\mathcal{U}_s(\mathcal{X}_s)$.

In the latter definition, a state trajectory in a period T, $\phi(t; x_s, u_s)$, for $t \in (0, T]$, uniquely defines an orbit o_s. More precisely, the orbit is given by the free response after the jump, $\phi(t; x_s, u_s) = e^{A_c t}(A_d x_s + B u_s)$, $t \in (0, T]$. The orbits $o_s(x_s, u_s)$, with $x_s \in \mathcal{X}_s$, are called equilibrium orbits. Figure 2 shows a schematic plot of some equilibrium orbits. Given that o_s is non-convex, a better characterisation of the generalised equilibrium can be done by defining its convex hull.

Definition 3.2 (Equilibrium orbits set of ICS): Consider a ICS (1) and a generalised control equilibrium set $\mathcal{X}_s$, together with the equilibrium input set $\mathcal{U}_s(\mathcal{X}_s)$. Then, the equilibrium orbits set of ICS, $\mathcal{X}_{\mathcal{O}_s}(\mathcal{X}_s) = \mathcal{X}_{\mathcal{O}_s}(\mathcal{X}_s, \mathcal{U}_s(\mathcal{X}_s))$, is given by

$$\begin{aligned}\mathcal{X}_{\mathcal{O}_s}(\mathcal{X}_s) &\triangleq \text{ch}\,\{\phi(t; x_s, u_s(x_s)), t \in [0, T],\ \forall\, x_s \in \mathcal{X}_s\} \\ &= \text{ch}\,\{o_s(x_s, u_s(x_s)),\ \forall\, x_s \in \mathcal{X}_s\}.\end{aligned} \tag{15}$$

Now, according to Definitions 3.1 and 3.2, it is clear that each equilibrium set of the primary underlying subsystem (10), $\mathcal{X}_s^\bullet$, is a (particular) generalised control equilibrium set.

Proposition 3.3: *Let $\mathcal{X}_s^\bullet \subseteq \mathcal{X}$ be a set of states $x_s^\bullet \in \mathcal{X}$ for which there exists an input $u_s = u_s(x_s^\bullet) \in \mathcal{U}$ such that $x_s^\bullet = A^\bullet x_s^\bullet + B^\bullet u_s(x_s^\bullet)$. Then $\mathcal{X}_s^\bullet$ is a generalised control equilibrium set of ICS with respect to the associated equilibrium orbit set, $\mathcal{X}_{\mathcal{O}_s}(\mathcal{X}_s^\bullet) = \mathcal{X}_{\mathcal{O}_s}(\mathcal{X}_s^\bullet, \mathcal{U}_s(\mathcal{X}_s^\bullet))$, where $\mathcal{U}_s(\mathcal{X}_s^\bullet) = \{u_s(x_s^\bullet) \in \mathcal{U} : x_s^\bullet \in \mathcal{X}_s^\bullet\}$.*

Proof: It is easy to see that for each $x_s^\bullet \in \mathcal{X}_s^\bullet$,

$$\begin{aligned}&\phi(T; x_s^\bullet, u_s(x_s^\bullet)) = A^\bullet(T) x_s^\bullet + B^\bullet(T) u_s(x_s^\bullet) = x_s^\bullet \in \mathcal{X}_s^\bullet, \\ &o_s(x_s^\bullet, u_s(x_s^\bullet)) \subseteq \mathcal{X}_{\mathcal{O}_s}(\{x_s^\bullet\}, \{u_s(x_s^\bullet)\}) \subseteq \mathcal{X}_{\mathcal{O}_s}(\mathcal{X}_s^\bullet).\end{aligned}$$

■

Condition $x_s^\bullet = A^\bullet x_s^\bullet + B^\bullet u_s(x_s^\bullet)$ implies that there is a state $x_s^\circ = x_s^\circ(x_s^\bullet) \triangleq A_d x_s^\bullet + B u_s(x_s^\bullet)$, such that $x_s^\circ = A^\circ x_s^\circ + B^\circ u_s(x_s^\bullet)$ (i.e. x_s° is an equilibrium of (11) associated to the same $u_s(x_s^\bullet)$).

Let us now introduce the counterpart of the generalised control equilibrium set, for the closed-loop ICS (7):

Definition 3.4 (Generalised equilibrium set of ICS): A set $\mathcal{X}_s$ is a generalised equilibrium set, with respect to $\bar{\Omega}$, for the closed-loop system (7), if $\mathcal{X}_s$ is a generalised control equilibrium set, with respect to $\bar{\Omega}$, for the open-loop system (1), with $u = \kappa(x)$.

3.3. Jump set

In many practical applications as, for instance, drug administration problems, the discrete-time transition matrix of ICS (1), A_d, is the identity matrix. In this case, (1) can be viewed as a continuous-time system, $\dot{x}(t) = A_c x(t) + B u(t)$, controlled by impulsive inputs. Let now $\mathcal{X}_s^\bullet$ be the maximal equilibrium set of the UDS (10) contained in $\mathcal{X}$. Given that system (1) is assumed to be controllable both UDS, (10) and (11) are also controllable. Then $\mathcal{X}_s^\bullet$ and $\mathcal{X}_s^\circ(\mathcal{X}_s^\bullet)$ are compact sets contained in subspaces of dimension m of $\mathbb{R}^n$ (Limon, Alvarado, Alamo, & Camacho, 2008), and it is possible to define:

Definition 3.5 (Jump set of ICS): The jump set of ICS (1) is given by the convex hull:

$$\mathcal{X}_s(\mathcal{X}_s^\bullet) \triangleq \text{ch}\left\{\mathcal{X}_s^\bullet, \mathcal{X}_s^\circ(\mathcal{X}_s^\bullet)\right\} \subseteq \mathbb{R}^n. \tag{16}$$

Next, the main property of $\mathcal{X}_s(\mathcal{X}_s^\bullet)$ is presented.

Proposition 3.6: *$\mathcal{X}_s(\mathcal{X}_s^\bullet)$ (and any subset of $\mathcal{X}_s(\mathcal{X}_s^\bullet)$ containing $\mathcal{X}_s^\bullet$) is a generalised control equilibrium set with respect to $\mathcal{X}_{\mathcal{O}_s}(\mathcal{X}_s(\mathcal{X}_s^\bullet))$, for system* (1).

Proof: It will be shown that any state $x_s \in \mathcal{X}_s(\mathcal{X}_s^\bullet)$ can be feasibly steered to a state $x_s^\circ(x_s^\bullet) \in \mathcal{X}_s^\circ(\mathcal{X}_s^\bullet)$ in a jump, and then, after the free response, it reaches a state $x_s^\bullet \in \mathcal{X}_s^\bullet \subseteq \mathcal{X}_s(\mathcal{X}_s^\bullet)$. By Definition 3.5, every state $x_s \in \mathcal{X}_s(\mathcal{X}_s^\bullet)$ - not lying in $\mathcal{R}(B)$) - can be expressed as $x_s = \alpha x_s^\bullet + (1-\alpha)x_s^\circ(x_s^\bullet)$, for some $x_s^\bullet \in \mathcal{X}_s^\bullet$ and some $\alpha \in \mathbb{R}$ (not necessarily positive). Furthermore, since $\mathcal{X}_s(\mathcal{X}_s^\bullet)$ is bounded (given that $\mathcal{X}_s^\bullet$ and $\mathcal{X}_s^\circ$ are bounded), $\alpha \in [\underline{\alpha}, \overline{\alpha}]$, for bounded minimal and maximal values, $\underline{\alpha}$ and $\overline{\alpha}$. So, if input $\hat{u} \triangleq \alpha u_s(x_s^\bullet)$ is injected to the system, then

$$\begin{aligned}\phi(T; x_s, \hat{u}) &= \mathrm{e}^{A_c T}\left(x_s + B\hat{u}\right)\\ &= \mathrm{e}^{A_c T}\left(\alpha x_s^\bullet + (1-\alpha)x_s^\circ(x_s^\bullet) + \alpha B u_s(x_s^\bullet)\right)\\ &= \mathrm{e}^{A_c T}\left((1-\alpha)x_s^\circ(x_s^\bullet) + \alpha x_s^\circ(x_s^\bullet)\right)\\ &= \mathrm{e}^{A_c T}x_s^\circ(x_s^\bullet) = x_s^\bullet \in \mathcal{X}_s(\mathcal{X}_s^\bullet), \end{aligned} \tag{17}$$

where the equalities follow from the facts that $x_s^\circ(x_s^\bullet) = x_s^\bullet + Bu_s(x_s^\bullet)$ and $\mathrm{e}^{A_c T}x_s^\circ(x_s^\bullet) = A^\bullet x_s^\circ(x_s^\bullet) = x_s^\bullet$. $\hat{u} = \alpha u_s(x_s^\bullet)$ is feasible, for $\alpha \in [\underline{\alpha}, \overline{\alpha}]$, because of the convexity of $\mathcal{U}$ and $\mathcal{X}_s(\mathcal{X}_s^\bullet)$. Finally, it is trivial that the trajectories starting in $x_s \in \mathcal{X}_s(\mathcal{X}_s^\bullet)$ will remain in$\mathcal{X}_{\mathcal{O}_s}(\mathcal{X}_s(\mathcal{X}_s^\bullet))$. ■

Remark 3.2 (Computation of $\mathcal{X}_{\mathcal{O}_s}(\mathcal{X}_s(\mathcal{X}_s^\bullet))$): In practical scenarios set $\mathcal{X}_{\mathcal{O}_s}(\mathcal{X}_s(\mathcal{X}_s^\bullet))$ can be approximated by the sampling in t of the map $S(t) \triangleq \mathrm{e}^{A_c t}\mathcal{X}_s^\circ(\mathcal{X}_s^\bullet)$. Also, it can be exactly over-approximated by a polytopic set, following methods as the one proposed in Darup (2015), which avoids the problem of selecting a sampling time for the approximation.

4. Closed-loop design

In this section the attractivity of the generalised equilibria under an impulsive feedback control law is defined and two new explicit control strategies are discussed.

4.1. Attractivity of the equilibrium sets

In this section some stability definitions of the generalised equilibria are presented. Based on Sopasakis et al. (2015), the attractivity of sets that not necessarily contain the origin can be defined as follows.

Definition 4.1 (Attractive sets): A nonempty, closed and convex set $\mathcal{X}_1 \subseteq \mathcal{X}$ is attractive for the closed-loop system (7), with respect to a (nonempty, closed and convex) set $\mathcal{X}_2 \supseteq \mathcal{X}_1$, with $\mathcal{X} \supseteq \mathcal{X}_2$, if there exists a vicinity of $\mathcal{X}_1$ such that $\lim_{k\to\infty} dist_{\mathcal{X}_1}(\phi(\tau_k; x_0, \kappa(\cdot))) = 0$, and $\lim_{t\to\infty} dist_{\mathcal{X}_2}(\phi(t; x_0, \kappa(\cdot))) = 0$, for all x_0 in such vicinity. If $\mathcal{X}_2 \equiv \mathbb{R}^n$, then $\mathcal{X}_1$ is called weakly attractive.

Weak attractivity only accounts for the closed-loop system (7) at the impulsive times, while attractivity also specifies a second set where the continuous-time trajectories between jumps converge. This makes sense given that the trajectories between jumps are free responses (nothing can be done until the next jump time) and they could escape. An asymptotic stability definition is also presented in Sopasakis et al. (2015), which basically requires the uniform boundedness of the solution trajectories. In this work, for the sake of simplicity, only the attractivity of the control strategy is considered.

Next, some results regarding the attractivity of the generalised equilibrium sets under a feedback control are presented.

Theorem 4.2: *Let $\mathcal{X}_s^{\bullet Tar}$ be an attractive set - in the usual sense of attractivity of discrete-time systems - for the closed-loop UDS* (10), *$x^\bullet(k+1) = A^\bullet x^\bullet(k) + B^\bullet \kappa(x^\bullet(k))$. Then, the generalised equilibrium set $\mathcal{X}_s^{Tar}(\mathcal{X}_s^{\bullet Tar})$ (or any subset of $\mathcal{X}_s^{Tar}(\mathcal{X}_s^{\bullet Tar})$ containing $\mathcal{X}_s^{\bullet Tar}$) is attractive for the closed-loop system* (7), *controlled by $\kappa(\cdot)$, with respect to $\mathcal{X}_{\mathcal{O}_s}^{Tar}(\mathcal{X}_s^{\bullet Tar})$.*

Proof: Assume that $\mathcal{X}_s^{\bullet Tar}$ is attractive for the UDS (10), controlled by $\kappa(\cdot)$, which means that there exists a vicinity of this set such that $\lim_{k\to\infty} x^\bullet(k) = x_s^\bullet$, for some $x_s^\bullet \in \mathcal{X}_s^{\bullet Tar}$. Then, given that $x^\bullet(k) \triangleq \phi(\tau_k; x_0, \kappa(\cdot))$, with $x^\bullet(0) = \phi(0; x_0, \kappa(\cdot)) = x_0$, and $\mathcal{X}_s^{\bullet Tar} \subseteq \mathcal{X}_s^{Tar}(\mathcal{X}_s^{\bullet Tar})$, it follows that $\lim_{k\to\infty} dist_{\mathcal{X}_s^{Tar}(\mathcal{X}_s^{\bullet Tar})}(\phi(\tau_k; x_0, \kappa(\cdot))) = 0$ (i.e. $\mathcal{X}_s^{Tar}(\mathcal{X}_s^{\bullet Tar})$ is weakly attractive). Furthermore, as $\lim_{k\to\infty} x^\bullet(k) = x_s^\bullet$ for some $x_s^\bullet \in \mathcal{X}_s^{\bullet Tar}$ then, by the continuity of the solution, the trajectories $tr(k) \triangleq \{\phi(t; x^\bullet(k), \kappa(x^\bullet(k))),\ t \in [\tau_k, \tau_{k+1})\}$ tend to the equilibrium orbit $o_s(x_s^\bullet, u_s(x_s^\bullet))$, associated to $x_s^\bullet \in \mathcal{X}_s^{\bullet Tar}$, as $k \to \infty$. By the definition of the equilibrium orbit set $\mathcal{X}_{\mathcal{O}_s}^{Tar}(\mathcal{X}_s^{\bullet Tar})$, then $o_s(x_s^\bullet, u_s(x_s^\bullet)) \subseteq \mathcal{X}_{\mathcal{O}_s}^{Tar}(\mathcal{X}_s^{\bullet Tar})$ for every $x_s^\bullet \in \mathcal{X}_s^\bullet$, which means that $\lim_{t\to\infty} dist_{\mathcal{X}_{\mathcal{O}_s}^{Tar}(\mathcal{X}_s^{\bullet Tar})}(\phi(t; x_0, \kappa(\cdot))) = 0$, and so $\mathcal{X}_s^{Tar}(\mathcal{X}_s^{\bullet Tar})$ is attractive with respect to $\mathcal{X}_{\mathcal{O}_s}^{Tar}(\mathcal{X}_s^{\bullet Tar})$ for the closed-loop system (7). ■

This result permits a flexible design of the controllers, since it means that steering the UDS (10) to its corresponding equilibrium region, $\mathcal{X}^{\bullet Tar}$, implies to steer the ICS (1) to $\mathcal{X}_{\mathcal{O}_s}^{Tar}(\mathcal{X}_s^{\bullet Tar}) \subseteq \mathcal{X}^{Tar}$.

Property 4.1: Let $tr_k(\cdot) : \mathcal{I} \to \mathbb{R}^n$, with $k \in \mathbb{N}$, the sequence of trajectories (functions of t) defined as $tr_k(t) \triangleq \phi(t; x_k, \kappa(x_k)) = \mathrm{e}^{A_c t}(x_k + B\kappa(x_k))$, with $\mathcal{I} = [a, T]$ for some $a > 0$.[1] If x_k converges to x_s as $k \to \infty$ and $\kappa(\cdot)$ is continuous w.r.t. x on $\mathcal{X}$, then $\lim_{k\to\infty} tr_k(t) = o_s(t)$, where $o_s(\cdot) : \mathcal{I} \to \mathbb{R}^n$ is defined as $o_s(t) \triangleq \phi(t; x_s, \kappa(x_s)) = \mathrm{e}^{A_c t}(x_s + Bu_s(x_s))$.

Proof: Given $\epsilon > 0$, there exists a scalar $N(\epsilon)$ (which does not depend on t, for uniform convergence), such that $\|tr_k(t) - o_s(t)\| < \epsilon$, for every $k > N(\epsilon)$.

As the sequence of states x_k converges to x_s, as $k \to \infty$, and the control law $\kappa(\cdot)$ is continuous w.r.t. x on $\mathcal{X}$, it is known that $\kappa(x_k) \to \kappa(x_s) = u_s$, as $k \to \infty$. This means that there exist $N_x(\tilde{\epsilon})$ and $N_\kappa(\tilde{\epsilon})$ such that $\|x_k - x_s\| < \tilde{\epsilon}$ and $\|\kappa(x_k) - x_s\| < \tilde{\epsilon}$, for an arbitrary $\tilde{\epsilon} > 0$, for every $k > \max\{N_x(\tilde{\epsilon}),\ N_\kappa(\tilde{\epsilon})\}$. Particularly, this holds for $\tilde{\epsilon} = \epsilon/M(1 + \|B\|)$. Then,

$$\begin{aligned} |tr_k(t) - o_s(t)| &= \left\| e^{A_c t} \left(x_k + B\kappa(x_k) - e^{A_c t}(x_s + Bu_s) \right) \right\| \\ &\leq \|e^{A_c t}\| \left(\|x_k - x_s\| + \|B\| \|\kappa(x_k) - u_s\| \right) \\ &\leq M\left(\tilde{\epsilon} + \|B\|\tilde{\epsilon}\right) = \epsilon, \end{aligned}$$

for any $k > N \triangleq \max\{N_x(\tilde{\epsilon}), N_\kappa(\tilde{\epsilon})\}$, where $M \triangleq \sup_{t\in(0,T]} \|e^{A_c t}\|$. Given that $\tilde{\epsilon}$ is a function of only ϵ (not of t), then $N = N(\epsilon)$. This shows the uniform convergence of $tr_k(t)$ to $o_s(t)$. ■

Remark 4.1: Notice that the key point to prove convergence is the continuity of $tr_k(t)$ w.r.t. x_k, in the sense that small distances in x_k corresponds to small distance between the corresponding functions.

This property ensures that any stabilising feedback control will steer the trajectories of the systems generated by the control law to the orbit equilibrium, and there will not be any escape of trajectories.

4.2. Affine feedback control

According to the control objective of steering the impulsive system to a non-zero equilibrium inside the target set $\mathcal{X}^{Tar}$, the following control law is introduced:

Theorem 4.3: *Consider an equilibrium $x_s^\circ \in \mathcal{X}_s^{\circ Tar} \subseteq \mathcal{X}^{Tar}$ and a period $T > 0$. Assume that the triplet (A_c, A_d, B) is controllable. Then, $x_s^\circ \in \mathcal{X}_s^{Tar}$ is attractive for system (7), with respect to $\mathcal{X}_{\mathcal{O}_s}^{Tar}$, applying the control law $\kappa(x(\cdot)) = -Kx(\cdot) + \zeta$, where parameters K and ζ are chosen to fulfil $\rho(F) < 1$ and $B\zeta = (I - F)x_s^\circ$, respectively, with $F = (A_d - BK)\, e^{A_c T}$.*

Proof: Consider the control law $\kappa(x(\tau_j)) = -Kx(\tau_j) + \zeta$ to stabilise the impulsive system (1) at the equilibrium $x_s^\circ \in \mathcal{X}_s^{\circ Tar} \subseteq \mathcal{X}^{Tar}$. Then, the discrete part of system (1) becomes

$$x(\tau_j^+) = (A_d - BK)x(\tau_j) + B\zeta, \quad j = 1, 2, \ldots. \tag{18}$$

The state response after p impulses results

$$\begin{aligned} x(\tau_p^+) = &\left(\prod_{i=1}^{p} (A_d - BK)\, e^{A_c T} \right) x_0 \\ &+ \sum_{j=1}^{p} \left(\prod_{i=1}^{p-j} (A_d - BK)\, e^{A_c T} \right) B\zeta. \end{aligned} \tag{19}$$

Since the impulses are periodically applied, Equation (19) reduces to

$$x(\tau_p^+) = F^p x_0 + \left(F^{p-1} + F^{p-2} + \cdots + F + I \right) B\zeta, \tag{20}$$

where $F \triangleq (A_d - BK)\, e^{A_c T}$. This is a geometric series based on the matrix F. Given that the triplet (A_c, A_d, B) is assumed controllable, the parameter K is chosen to fulfil $\rho(F) < 1$, which means that the geometric series converges to $(I - F^p)(I - F)^{-1}$ and Equation (20) becomes

$$x(\tau_p^+) = F^p x_0 + (I - F^p)(I - F)^{-1} B\zeta. \tag{21}$$

Since the goal is to asymptotically steer the system to the equilibrium x_s°, it is required that

$$\lim_{p\to\infty} \|x(\tau_p^+) - x_s^\circ\| = 0. \tag{22}$$

Now, replacing $x(\tau_p^+)$ by Equation (21) in (22), it follows that

$$\lim_{p\to\infty} \|F^p x_0 + (I - F^p)(I - F)^{-1} B\zeta - x_s^\circ\| = 0 \tag{23}$$

and, since K was chosen such that $\rho(F) < 1$, then $F^p \to 0$ as $p \to \infty$, which implies that

$$\lim_{p\to\infty} \|x(\tau_p^+) - x_s^\circ\| = \|(I - F)^{-1} B\zeta - x_s^\circ\|. \tag{24}$$

If ζ is chosen to fulfil $B\zeta = (I - F)x_s^\circ$, then $\lim_{p\to\infty} \|x(\tau_p^+) - x_s^\circ\| = 0$, as it is desired. Now, given that $x_s^\circ \in \mathcal{X}_s^{\circ Tar} \subseteq \mathcal{X}_s^{Tar}$, according to Definition 3.2 and Theorem 4.2, $\mathcal{X}_s^{Tar}$ is attractive for the closed-loop system with respect to $\mathcal{X}_{\mathcal{O}_s}^{Tar}$. ■

Notice that according to Xie and Wang (2005), the controllability of the triplet (A_c, A_d, B) implies that there exists a feedback K such the closed-loop system eigenvalues can be placed in arbitrary locations. Besides, if the underlying discrete system (10) is such that the rank of $[\lambda I - A^\bullet, B^\bullet]$ is n, for all $\lambda \in \mathbb{C}$, then such an eigenvalue placement problem can be solved by standard methods.

Remark 4.2: Consider the system (7), and the feedback $\kappa(x(\cdot)) = -Kx(\cdot) + \zeta$. If the output is affected directly by the input, then the feedback gains can be chosen as $\zeta = ((CB)'CB)^{-1}CB$, and $K = \zeta C$.

Remark 4.3: Consider the system (7), $n=1$, the feedback $\kappa(x(\cdot)) = -kx(\cdot) + \zeta$, $\eta \in [0,1]$, and $\epsilon \in \mathbb{R}_+$. If $k > (A_d - \mathrm{e}^{-A_c T})/B$, $\zeta = ((1-V)x_s^\circ/B)(1-\eta(1-\mathrm{e}^{A_c T}))$, and $T \leq (1/\|A\|)\log(\mathsf{sgn}(A_c)\epsilon + 1)$, then $x_s^\circ \in \mathcal{X}_s^{Tar}$ is attractive for system (7) with respect to $\mathcal{X}_{\mathcal{O}_s}^{Tar}$, the systems is stabilised at $\hat{x} = \eta x_s^{-1\bullet} + (1-\eta)x_s^\circ$, and $\|\phi_{cl}(t)\| \leq \epsilon$, for $t \in (0, T]$.

4.3. Optimal feedback control

The common method to design a state feedback is by solving a pole placement problem, as it was stated above. However, a more challenging choice is to select the feedback according to the optimal control theory, in which a general objective function is minimised. Next, it is shown that the solution of the infinite continuous-time optimal control problem - subject to an impulsive system - can be obtained by solving a discrete-time optimisation problem associated to the UDS.

The idea is to minimise the cost function

$$J(x,u) = \int_0^\infty \left\{x(t)'Qx(t) + u(t)'Ru(t)\right\} \mathrm{d}t, \tag{25}$$

subject to

$$\begin{array}{lll} \dot{x}(t) & = A_c x(t), \quad x(0) = x_0, & t \neq \tau_k, \\ x(\tau_k^+) & = A_d x(\tau_k) + Bu(\tau_k), & k \in \mathbb{N}, \end{array}, \tag{26}$$

where $Q \geq 0$ and $R > 0$ are the state and control weighting matrices, respectively.

The above problem is the linear quadratic regulator (LQR) based on an impulsive system. The closed-loop system derived from the latter formulation steers the state to the origin, as it is stated in the following Proposition:

Proposition 4.4: *Assume that the triplet (A_c, A_d, B) is controllable. Then, the solution of the problem*(25)–(26) *is an impulsive feedback control, $u(\tau_k) = Kx(\tau_k)$, with $K = ((B^\bullet)'PB^\bullet + \tilde{R})^{-1}(A^\bullet PB^\bullet + \tilde{S})'$, where P is the solution of the impulsive discrete-time algebraic Riccati equation* (*iDARE*)

$$\begin{aligned} P = \tilde{Q} + (A^\bullet)'PA^\bullet - ((A^\bullet)'PB^\bullet + \tilde{S})((B^\bullet)'PB^\bullet \\ + \tilde{R})^{-1}((A^\bullet)'PB^\bullet + \tilde{S})', \end{aligned} \tag{27}$$

and

$$\tilde{Q} = A_d' Q_1 A_d, \quad \tilde{R} = R + B'Q_1 B, \quad \tilde{S} = A_d Q_1 B, \tag{28}$$

with $Q_1 = \int_0^T \mathrm{e}^{A'\theta} Q \mathrm{e}^{A\theta}\, \mathrm{d}\theta$ *and* $\begin{pmatrix} \tilde{Q} & \tilde{S} \\ \tilde{S}' & \tilde{R} \end{pmatrix} > 0$.

Proof: Note that the cost function J can be written as

$$J = \sum_{i=0}^\infty \int_{\tau_i^+}^{\tau_{i+1}} \left\{x(t)'Qx(t) + u(t)'Ru(t)\right\} \mathrm{d}t. \tag{29}$$

Now, taking into account that during the interval $(\tau_i, \tau_{i+1}]$ the state solution verifies $x(t) = \mathrm{e}^{A_c(t-\tau_i)}(A_d x(\tau_i) + Bu(\tau_i))$, the integral $J_i = \int_{\tau_i^+}^{\tau_{i+1}} \{x(t)'Qx(t) + u(t)'Ru(t)\}\, \mathrm{d}t$ becomes

$$\begin{aligned} J_i = \int_{\tau_i^+}^{\tau_{i+1}} \Big\{ (\mathrm{e}^{A_c(t-\tau_i)}(A_d x(\tau_i) + Bu(\tau_i))' Q\, \mathrm{e}^{A_c(t-\tau_i)} \\ \times (A_d x(\tau_i) + Bu(\tau_i)) + u(t)'Ru(t)\delta(t-\tau_i) \Big\}\, \mathrm{d}t, \end{aligned} \tag{30}$$

where δ stands for the Dirac function. After some algebraic manipulations, J_i reads

$$\begin{aligned} J_i = \int_{\tau_i^+}^{\tau_{i+1}} \Big\{ & x(\tau_i)' A_d'\, \mathrm{e}^{A_c'(t-\tau_i)} Q\, \mathrm{e}^{A_c(t-\tau_i)} A_d x(\tau_i) \\ & + 2x(\tau_i)' A_d'\, \mathrm{e}^{A_c'(t-\tau_i)} Q\, \mathrm{e}^{A_c(t-\tau_i)} Bu(\tau_i) \\ & + u(\tau_i)' B'\, \mathrm{e}^{A_c'(t-\tau_i)} Q\, \mathrm{e}^{A_c(t-\tau_i)} Bu(\tau_i) \Big\}\, \mathrm{d}t \\ & + u(\tau_i)' Ru(\tau_i). \end{aligned} \tag{31}$$

Now, distributing the integral and defining $Q_1 = \int_{\tau_i^+}^{\tau_{i+1}} \mathrm{e}^{A_c'(t-\tau_i)} Q\, \mathrm{e}^{A_c(t-\tau_i)}\, \mathrm{d}t = \int_0^T \mathrm{e}^{A_c'\theta} Q\, \mathrm{e}^{A_c\theta}\, \mathrm{d}t$, J_i results

$$J_i = x(\tau_i)'\tilde{Q}x(\tau_i) + 2x(\tau_i)'\tilde{S}u(\tau_i) + u(\tau_i)'\tilde{R}u(\tau_i). \tag{32}$$

where $\tilde{Q} = A_d' Q_1 A_d$, $\tilde{R} = R + B'Q_1 B$, $\tilde{S} = A_d Q_1 B$. Introducing the last equation into Equation (29), the problem (25)–(26) is transformed into an infinite discrete-time optimal control problem, where the cost function

$$J = \sum_{i=0}^\infty x^\bullet(i)'\tilde{Q}x^\bullet(i) + 2x^\bullet(i)'\tilde{S}u^\bullet(i) + u^\bullet(i)'\tilde{R}u^\bullet(i). \tag{33}$$

is minimised subject to the primary underlying discrete-time subsystem

$$x^\bullet(j+1) = A^\bullet x^\bullet(j) + B^\bullet u^\bullet(j), \quad x^\bullet(0) = x(\tau_0). \tag{34}$$

As it is well-known, given that the triplet (A_c, A_d, B) is controllable, the solution of this problem is obtained by solving the corresponding DARE (27), and the resulting control law is $u(\tau_k) = u^\bullet(k) = Kx^\bullet(k) = Kx(\tau_k)$, with $K = ((B^\bullet)'PB^\bullet + \tilde{R})^{-1}(A^\bullet PB^\bullet + \tilde{S})'$. ■

Remark 4.4: Note that the latter result can be extended to the non-zero regulation problem by considering a new state $x_e = r - Cy$ (where r is the non-zero set-point), the

extended system with matrices $A_e = \left(\begin{smallmatrix} A^\bullet & 0 \\ -C & 0 \end{smallmatrix}\right)$, $B_e = \left(\begin{smallmatrix} B^\bullet \\ 0 \end{smallmatrix}\right)$, and penalising matrices Q and R of the appropriated dimensions.

Next, the main Theorem of the subsection, showing the attractivity of the closed-loop under the optimal control law is provided.

Theorem 4.5: *Consider an equilibrium $x_s^\circ \in \mathcal{X}_s^{\circ Tar} \subseteq \mathcal{X}^{Tar}$ and a period $T > 0$. Assume that the triple (A_c, A_d, B) is controllable. Then, $x_s^\circ \in \mathcal{X}_s^{Tar}$ is attractive for system (7), with respect to $\mathcal{X}_{\mathcal{O}_s}^{Tar}$, applying the control law $\kappa(x(\cdot)) = -Kx(\cdot) + \zeta$, where parameters K and ζ are obtaining from the solution of the extended iDARE equation.*

Proof: It is straightforward from Proposition 4.4 and Remark 4.4. ■

Finally, an algorithm is provided to compute the optimal feedback parameters.

(1) Verify that the triplet (A_c, A_d, B) is controllable.
(2) Choose the penalising matrices Q and R.
(3) Compute the matrices of the underlying subsystem $A^\bullet$ and $B^\bullet$, and their extended versions A_e and B_e.
(4) Compute the matrices of the iDARE, $\tilde{Q}$, $\tilde{R}$, and $\tilde{S}$.
(5) Finally, solve the iDARE to obtain the feedback gain $\hat{K}$. Then, $K = [\hat{K}_1 \cdots \hat{K}_n]$ and $\zeta = \hat{K}_{n+1}$, where $\hat{K}_i$ its ith element of $\hat{K}$.

5. Numerical examples

5.1. Example 1: lithium ions distribution in the human body

In Ehrlich et al. (1980) a physiological pharmacokinetic model based on experimental data, which describes the distribution of Lithium ions in the human body upon oral administration, is provided. The system state vector is given by $x(t) = [C_P(t)\ C_{RBC}(t)\ C_M(t)]^{\mathrm{T}}$, where $C_P(t)$ is the concentration of plasma (P), $C_{RBC}(t)$ is the concentration of the red blood cells (RBC), and $C_M(t)$ is the concentration of muscle cells (M). All these concentrations are given in n mol/L. The input u is given by the amount of the dose, in *nmol*. The administration period is initially fixed in $T = 3$ h. The dynamics of the drug distribution is described by an ICS as in (1), characterised by the matrices

$$A_c = \begin{pmatrix} -0.6137 & 0.1835 & 0.2406 \\ 1.2644 & -0.8 & 0 \\ 0.2054 & 0 & -0.19 \end{pmatrix},$$

$$B = \begin{pmatrix} 10.9 \\ 0 \\ 0 \end{pmatrix}, \quad A_d = I_{3x3}. \tag{35}$$

The state window target is defined by $\mathcal{X}^{Tar} = \{x : [0.4\ 0.6\ 0.5]^{\mathrm{T}} \preceq x \preceq [0.6\ 0.9\ 0.8]^{\mathrm{T}}\}$, as it is described in Ehrlich et al. (1980) and Sopasakis et al. (2015).

The maximal intake period T for the given therapeutic window $\mathcal{X}^{Tar}$ is given by $T_{\max} = 6$ h. In fact, for larger periods the set containing all the orbits starting at $\mathcal{X}_s^{\bullet Tar}$, $\mathcal{X}_{\mathcal{O}_s}^{Tar}(\mathcal{X}_s^{\bullet Tar})$ is not contained in $\mathcal{X}^{Tar}$ (which was checked by simulation). This analysis provides a practical way to find the maximal value of T, according to control system specifications. The intake period was then selected to be $T = 3$ h.

To implement the impulsive affine feedback control of Theorem 4.3, it is necessary to compute K and ζ. K was chosen by solving a standard eigenvalue placement problem (Yang, 2001), and its value is $K = (0.05\ 0.01\ 0.02)$. The spectral radius was approximately 0.6807. The value$\zeta \approx 0.0513$ was computed from $B\zeta = (I - F)x_s^\circ$, with $x_s^\circ = (0.57\ 0.78\ 0.55)$ and $u_s = 0.89$. The input time evolution is shown in Figure 3 (blue) while the state evolution is shown in 4 (blue). The performance of the second method is also illustrated in Figures 3 and 4, red line. To compute the feedback parameters, $Q = I_{3\times 3}$, $R = 2$ were chosen. As the penalty matrix R is bigger than Q, the control action results smaller than the produced by the method 1 (pole placement). However, both strategies steer the state to the desired non-zero set-point.

Given that one of the main advantages of the proposed controller is its simplicity - mainly in contrast to other model-based controller - a constrained impulsive MPC controller (based on Rivadeneira et al., 2015; Sopasakis et al., 2015) is also simulated. Figures 3 and 4 (black line)

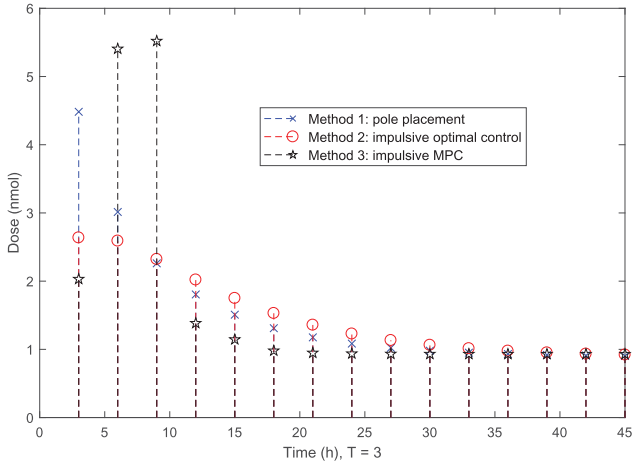

Figure 3. Input time evolution. Method 1: pole placement feedback control, blue line; Method 2: impulsive optimal control, red line; and impulsive MPC, black line.

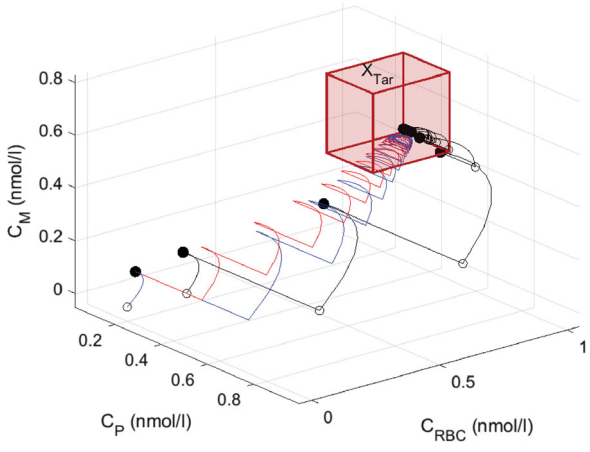

Figure 4. State time evolution. Method 1: pole placement feedback control, blue line; Method 2: impulsive optimal control, red line; and impulsive MPC, black line.

also show the input and state time evolutions corresponding to this controller. As it can be seen, the performance of the feedback controller is satisfactory, while the state and control constraints are not violated. As it is desired, both controllers are able to steer the state to the therapeutic window, in a relatively short time. Besides, the input makes the main effort at the beginning, and after its settling time it remains approximately constant around the desired equilibrium value u_s.

The results presented here can be extended to follow time variant trajectories as it is shown in Figures 5–6. In some biomedical applications it is necessary to enclosed the behaviour of one state between two known boundaries (see Tilbury, Felt, Kaciroti, Wang, & Tardif., 2008). The strategies envisioned here can tackle this situation. For example, two time variant known bounds are added to the first state, the goal is that the output behaviour remains surrounded by the two trajectories (in this case a sine and cosine). To do this, the same affine feedback tuned before was used, but the affine part was calculated to compensate the new reference. This value was $\zeta = 0.0912$. This way the system follow the upper bound imposed. To track the lower bound, the switching time (impulsive time instant) is used as a second input, and it was forced to verify $y(\tau_k) = z_2(\tau_k)$, where z_2 is the lower bound. For this example, this strategy works, but the whole situation must be further analysed in a specialised case-study.

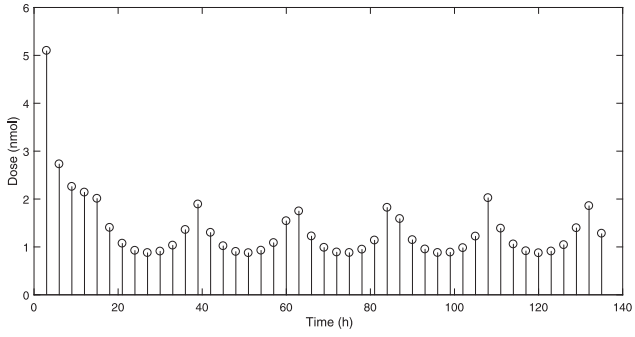

Figure 6. Control trajectory with lower and upper time variant constraints.

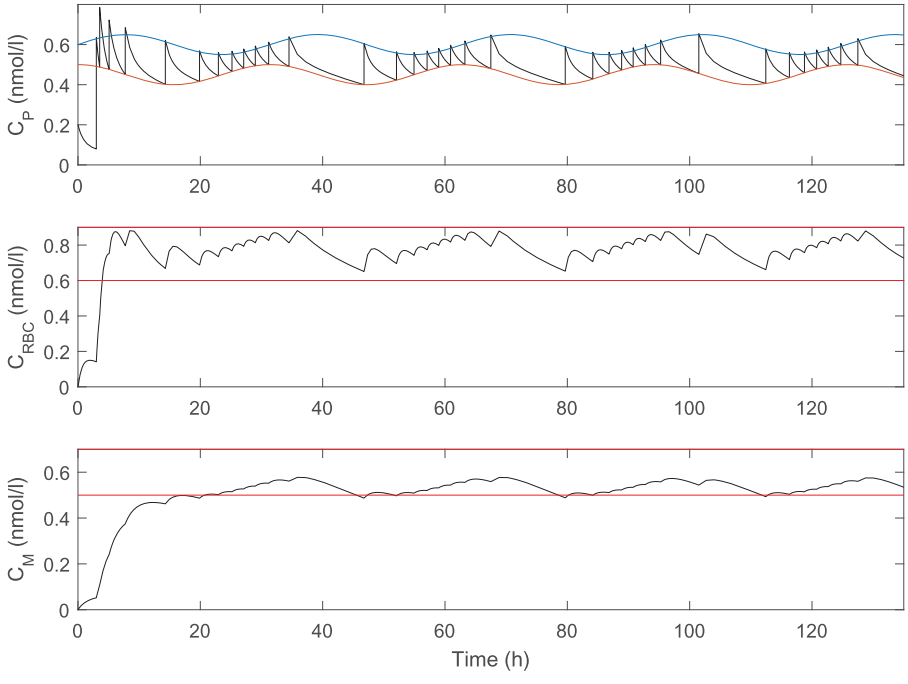

Figure 5. State evolution with lower and upper time variant constraints.

5.2. Example 2: HIV infection dynamics with treatment

The second example is taken from Rivadeneira and Moog (2012), a '3D HIV model' (defined by T, y, z) which describes the virus infection dynamics and incorporates the effect of drug intake (w, u) (Legrand et al., 2003; Mhawej, Moog, Biafore, & Brunet-Francois, 2010). The completed impulsive model is given by:

$$\begin{aligned}
\dot{T}(t) &= s - \delta T(t) - \beta T(t) z(t),\\
\dot{y}(t) &= \beta T(t) z(t) - \mu y(t),\\
\dot{z}(t) &= \left(1 - \frac{w(t)}{w(t) + w_{50}}\right) k y(t) - c z(t), \qquad (36)\\
\dot{w}(t) &= -K_w w(t),\\
w(\tau_k^+) &= w(\tau_k) + u(\tau_k), \quad k \in \mathbb{N},
\end{aligned}$$

where healthy CD4 cells T are produced from the thymus at a constant rate s (cells mm^{-3} day^{-1}) and die with a half life time equal to $1/\delta$ (day). The healthy cells are infected by the virus at a rate that is proportional to the product of their population and the amount of free virus particles. Constant β (ml copies^{-1} day^{-1}) indicates the effectiveness of the infection process. The infected CD4+ cells (y) result from the infection of healthy CD4 cells and die at a rate μ (day^{-1}). Free virus particles (z) are produced from infected CD4 cells at a rate k (copies cells^{-1} mm^{-3} ml^{-1} day^{-1}) and die within a half life time equal to $1/c$ (day). The pharmacokinetics and pharmacodynamics phases of the drug administration are related to w (the amount of drug in the body at time t) and $\eta = w(t)/w(t) + w_{50}$ (the efficacy of an anti-HIV treatment, where w_{50} is the concentration of drug that lowers the viral load by 50%). Although a cocktail of drugs is generally used, only Zidovudine therapies will be considered. The model parameters are given by: $s = 9$, $\delta = 0.009$, $\beta = 4e-6$, $\mu = 0.3$, $k = 80$, $c = 0.6$, $K_w = 8.4$ (day), $w_{50} = 89.6$ (mg) (see Rivadeneira & Moog, 2012 for details).

This model has two equilibria, the first one (or the 'healthy' equilibrium) characterised by the absence of virus, i.e. $(T_h, y_h, z_h, w_h) = (\lambda/\delta, 0, 0, 0)$, and the second one (or the 'endemic' equilibrium) dominated by a virus concentration $(T_e, y_e, z_e, w_e) = ((u_e + w_{50}K_w)\mu c / \beta\kappa w_{50}K_w, (s - \delta T_e)/\mu, w_{50}K_w\kappa y_e/c(u_e + w_{50}K_w), u_e/K_w)$. Notice that for $u_e = 0$ (equilibrium control), the maximum virus concentration is achieved.

To design both impulsive control strategies described previously, the system is linearised around the endemic equilibrium. The resulting matrices A_c and B are:

$$A_c = \begin{pmatrix} -\delta z_e & 0 & -\beta T_e & 0 \\ \beta z_e & -\mu & \beta T_e & 0 \\ 0 & \dfrac{k w_{50}}{w_e + w_{50}} & -c & \dfrac{-k w_{50} y_e}{(w_e + w_{50})^2} \\ 0 & 0 & 0 & -K_w \end{pmatrix},$$

$$B = \begin{pmatrix} 0 \\ 0 \\ 0 \\ 1 \end{pmatrix},$$

The selected intake period is $T = 0.5$ day. The state and input constraints are imposed as $\mathcal{X} = \{x : [0\ 0\ 0\ 0]^{\mathrm{T}} \preceq x \preceq [1000\ 20\ 1500\ 100]^{\mathrm{T}}\}$ and $\mathcal{U} = \{u : 0 \le u \le 450\}$, respectively. The state window target is defined by $\mathcal{X}^{Tar} = \{x : [900\ 0\ 0\ 0]^{\mathrm{T}} \preceq x \preceq [1000\ 5\ 250\ 60]^{\mathrm{T}}\}$. As it is described in Rivadeneira and Moog (2012), the control goal is to steer the system from the endemic equilibrium to a healthy zone defined by $\mathcal{X}^{Tar}$. Besides, the anti-HIV treatment is considered successful if z is below the threshold of 50 copies/ml. These two objectives are represented by the therapy or target window. However, this set should be determined by the treating physician.

According to Theorem 4.3, K and ζ can be computed as the impulsive system is controllable. K is selected by a standard eigenvalue placement problem (Yang, 2001), and its value is $K = [0.0349\ \ 33.8248\ \ -0.8414\ \ 0.9876]$. The spectral radius was approximately 0.92, which ensures attractivity. ζ is computed from the condition $B\zeta = (I - F)x_s^{\circ}$, with $x_s^{\circ} = [968.3053\ 0.3636\ 29.5146\ 52.2726]$ and its value is 4500. The state and input time evolutions are shown in Figure 7 (blue circles and dotted line).

Also for comparison a MPC controller is tuned as: $N = 35$, $Q = \mathrm{diag}([1\ 1\ 1\ 1])$, $R = 0.1$ and $p = 10000$ based on Rivadeneira et al. (2015). Figure 7 (black stars and solid line) shows the state and input time evolutions. The impulsive feedback for the HIV example does not generate a feasible control at the beginning; its values are beyond the medical constraint settled in 450 mg of drug. This forces to saturate the doses, which is not a recommended practice. However, this situation has not a great impact in the overall performance, and the simplicity of the feedback remains being its main feature.

Other behavioural difference between the two control strategies is that the impulsive feedback injects to the system a bigger amount of drug, to compensate the elevated initial virus concentration. On the other hand, MPC is more conservative because of its well-known anticipative properties. This way, the feedback fulfils the medical goal of steering the virus concentration below the threshold of 50 copies/ml faster than the MPC. However, it should be

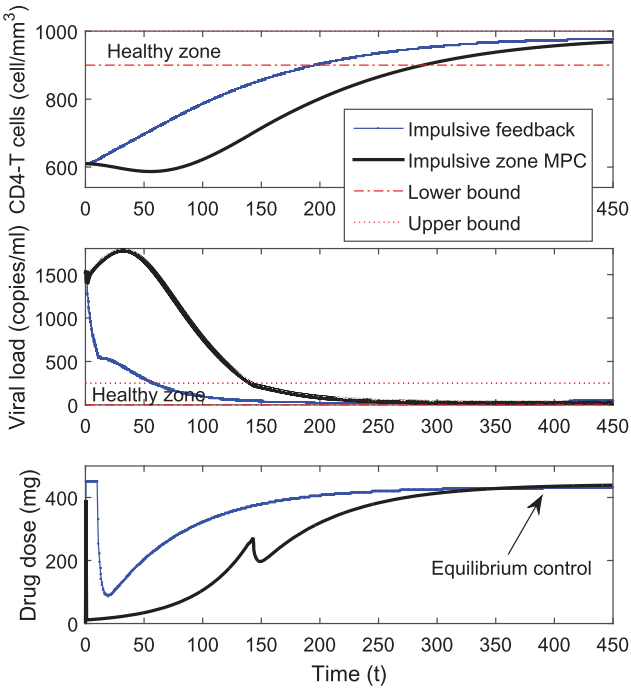

Figure 7. State time evolution. Feedback control, blue line; MPC, black line.

emphasised that an excessive amount of drug can produce dangerous side-effects on the patient (Costanza, Rivadeneira, Biafore, & D'Attellis, 2010). On the whole, this situation must be analysed more deeply in an adequate framework and it will be certainly studied in future works.

6. Conclusions

In this work, the non-zero set-point regulation problem of a linear impulsive system has been tackled. To this aim, the impulsive system dynamic was characterised by means of two discrete-time underlying subsystems, that allow not only to cope with the transient impulsive behaviour but also to define generalised equilibrium regions out of the origin. The idea is to determine these regions in such a way that they contain both, the discontinuities (jumps) and the free responses of the system, once it reaches a pure periodic behaviour. Based on the latter framework two feedback controllers were proposed, and the necessary-sufficient conditions for stability were provided. The benefits of the proposal were finally tested in two biomedical applications, which naturally incorporate the impulsive scheme. Future works include the study of impulsive systems with variable impulse times, in order to cope more efficiently with drug administration applications, such as HIV, influenza, cancer and other similar diseases.

Note

1. We consider here, for simplicity, the fixed time interval $\mathcal{I}$ instead of $(\tau_k, \tau_{k+1}]$ because $\tau_{k+1} - \tau_k = T$ for all $k \in \mathbb{N}$

Disclosure statement

No potential conflict of interest was reported by the authors.

Notes on contributors

Pablo S. Rivadeneira was born in Ipiales, Colombia in 1981. He received the Control Engineering degree from the Universidad Nacional de Colombia, at Medellín, in 2005, and the doctorate in Chemical Technology from the Universidad del Litoral, at Santa Fe, Argentina in 2010. After that, he did a postdoctoral stage at IRRCyN, Nantes, France during 2010–2012. Now, he is assistant professor at Universidad Nacional de Colombia. His main research interests include aspects of nonlinear systems and control, with applications to industrial and biological processes.

Alejandro H. González is a Titular Professor of Industrial Engineering at National University of Litoral (UNL), and Adjoint Researcher at the Argentine National Scientific and Technical Research Council (CONICET). After getting his Ph.D from UNL in 2006, he became Postdoctoral fellow at the Chemical Engineering Department at Universidade de São Paulo, São Paulo-Brazil, under the supervision of Prof. Darci Odloak (2007–2008) and, subsequently, at the "Departamento de Ingeniería y Automática de la Escuela Técnica Superior de Ingenieros de la Universidad de Sevilla, Seville-Spain (2010–2011). After concluding his Postdoctoral activities, he returned to Argentine to work as a researcher in the Process Control Group of INTEC (CONICET-UNL) and Professor at the University, as well as to supervise Ph.D. research projects and students at INTEC (CONICET-UNL). His research interests include Advanced Control, Model Predictive Control (MPC) design, Control of Constrained System and Invariant Sets for Linear Systems.

ORCID

Pablo S. Rivadeneira http://orcid.org/0000-0001-8392-4556

References

Bellman, R. (1971). Topics in pharmacokinetics, III: Repeated dosage and impulsive control. *Mathematical Biosciences*, *12*(1–2), 1–5.

Boianelli, A., Sharma-Chawla, N., Bruder, D., & Hernandez-Vargas, E. A. (2016, June). Oseltamivir PK/PD modeling and simulation to evaluate treatment strategies against Influenza-Pneumococcus coinfection. *Frontiers in Cellular and Infection Microbiology*, *6*(60), 1–11.

Chang, H., Astolfi, A., Moog, C. H., & Rivadeneira, P. S. (2014). A control systems analysis of HIV prevention model using impulsive input. *Biomedical Signal Processing and Control*, *13*, 123–131.

Chang, H., Astolfi, A., & Shim, H. (2011). A control theoretic approach to malaria immunotherapy with state jumps. *Automatica*, *47*, 1271–1277.

Chen, T., Kirkby, N. F., & Jena, R. (2012). Optimal dosing of cancer chemotherapy using model predictive control and moving horizon state/parameter estimation. *Computers Methods and Programs in Medicine*, *108*, 973–983.

Chen, Y., & Tian, R. (2013). Impulsive tracking control for non-measurable state with time-delay. *Journal of Networks*, *8*(4), 851–857.

Costanza, V., Rivadeneira, P. S., Biafore, F. L., & D'Attellis, C. E. (2010). Taking side effects into account for HIV medication. *IEEE Transactions on Biomedical Engineering*, *57*(9), 2079–2089.

Darup, M. S. (2015, December). Efficient constraint adaptation for sampled linear systems. In *Proceedings of the IEEE conference on decision and control* (pp. 15–18). Osaka.

Ehrlich, B. E., Clausen, C., & Diamond, J. M. (1980). Lithium pharmacokinetics: Single-dose experiments and analysis using a physiological model. *Journal of Pharmacokinetics and Biopharmaceutics*, *8*(5), 439–461.

Fraga, S. (2013). *Impulsive feedback control: A constructive approach* (Doctoral Thesis). Universidade do Porto.

Huang, M., Li, J., Song, X., & Guo, H. (2012). Modeling impulsive injections of insulin: Towards artificial pancreas. *SIAM Journal on Applied Mathematics*, *72*(5), 1524–1548.

Legrand, M., Comets, E., Aymard, G., Tubiana, R., Katlama, C., & Diquet, B. (2003). An in vivo pharmacokinetic/pharmacodynamic model for antiretroviral combination. *HIV Clinical trials*, *4*(3), 170–183.

Limon, D., Alvarado, I., Alamo, T., & Camacho, E. F. (2008). MPC for tracking piecewise constant references for constrained linear systems. *Automatica*, *44*(9), 2382–2387.

Luo, R., Piovoso, M. J., Martinez-Picado, J., & Zurakowski, R. (2011). Optimal antiviral switching to minimize resistance risk in HIV therapy. *PLoS ONE*, *6*(11), e27047.

Mhawej, M., Moog, C., Biafore, F., & Brunet-Francois, C. (2010, January). Control of the HIV infection and drug dosage. *Biomedical Signal Processing and Control*, *5*(1), 45–52.

Ortega, J. M. (1987). *Matrix theory. A second course* (1st ed.). New York: Plenum Press.

Pierce, J. G., & Schumitzky, A. (1976). Optimal impulsive control of compartment models, I: Qualitative aspects. *Journal of Optimization Theory and Applications*, *18*, 537–554.

Rivadeneira, P. S., Caicedo, M., Ferramosca, A., & González., A. H. (2017). Impulsive zone model predictive control (IZMPC) for therapeutic treatments: Application to HIV dynamics. In *Proceedings of the 56th IEEE conference on decision and control* (pp. 4094–4099). Melbourne.

Rivadeneira, P. S., Ferramosca, A., & González, A. H. (2015). MPC with state window target control in linear impulsive systems. *IFAC-PapersOnLine*, *48*(23), 507–512.

Rivadeneira, P. S., Ferramosca, A., & Gonzalez, A. H. (2016). Impulsive zone model predictive control with application to type I diabetic patients. In *Proceedings of the 2016 IEEE multi-conference on systems and control* (pp. 544–549). Buenos Aires.

Rivadeneira, P. S., & Moog, C. H. (2012). Impulsive control of single-input nonlinear systems with application to HIV dynamics. *Applied Mathematics and Computation*, *218*(17), 8462–8474.

Sopasakis, P., Patrinos, P., Sarimveis, H., & Bemporad, A. (2015). Model predictive control for linear impulsive systems. *IEEE Transactions on Automatic Control*, *60*, 2277–2282.

Tang, B., & Xiao, Y. (2016). A feedback control model of comprehensive therapy for treating immunogenic tumours. *International Journal of Bifurcation and Chaos*, *26*(3), 1–22.

Tilbury, D. M., Felt, B. T., Kaciroti, N., Wang, L., & Tardif., T. (2008, October). Dynamic systems modeling of cortisol stress response. In *Proceedings of the ASME dynamic systems and control conference* (pp. 1–8). Michigan.

Wei, C., Zhang, S., & Chen, L. (2013). Impulsive state feedback control of cheese whey fermentation for single-cell protein production. *Journal of Applied Mathematics*, *2013*(Article ID 354095), 1–10.

Xie, G., & Wang, L. (2005). Controllability and observability of a class of linear impulsive systems. *Journal of Mathematical Analysis and Applications*, *304*, 336–355.

Yang, T. (2001). *Impulsive control theory* (1st ed.). *LNCIS*. Berlin, Heidelberg: Springer-Verlag.